Transport properties of antidot superlattices of graphene nanoribbons

Article *in* Physical Review B · August 2009

DOI: 10.1103/PhysRevB.80.073402

6 authors, including:

Luis Rosales
Universidad Técnica Federico Santa María
29 PUBLICATIONS **743** CITATIONS
SEE PROFILE

Monica Pacheco
Universidad Técnica Federico Santa María
125 PUBLICATIONS **1,512** CITATIONS
SEE PROFILE

Alejandro Leon
Universidad Diego Portales
25 PUBLICATIONS **117** CITATIONS
SEE PROFILE

Andrea Latgé
Universidade Federal Fluminense
144 PUBLICATIONS **2,038** CITATIONS
SEE PROFILE

Transport properties of antidot superlattices of graphene nanoribbons

L. Rosales,[1,5] M. Pacheco,[1,*] Z. Barticevic,[1] A. León,[2] A. Latgé,[3] and P. A. Orellana[4]
[1]*Departamento de Física, Universidad Santa María, Casilla 110 V, Valparaíso, Chile*
[2]*Facultad de Ingeniería, Universidad Diego Portales, Casilla 8370179, Santiago, Chile*
[3]*Instituto de Física, Universidade Federal Fluminense, Niterói, Rio de Janeiro 24210-340, RJ, Brazil*
[4]*Departamento de Física, Universidad Católica del Norte, Casilla 1280, Antofagasta, Chile*
[5]*Instituto de Física, Pontificia Universidad Católica de Valparaíso, Casilla 4059, Valparaíso, Chile*
(Received 3 April 2009; revised manuscript received 3 July 2009; published 7 August 2009)

In this work we show a theoretical study of the electronic and transport properties of superlattices formed by a periodic structure of vacancies (antidots) on graphene nanoribbons. The systems are described by a single-band tight-binding Hamiltonian and also by *ab initio* total energy density-functional theory calculations. The quantum conductance is determined within the Green's function formalism, calculated by real-space renormalization techniques. A series of well defined gap structures on the conductance as a function of the Fermi energy is observed. This strongly depends on the period of the vacancies on the nanoribbon and on the internal geometrical structure of the supercell. Controlling these parameters could be possible to modulate the electronic response of the systems.

DOI: 10.1103/PhysRevB.80.073402 PACS number(s): 73.63.−b, 73.22.−f

The special electronic behavior and the room-temperature mechanical stability exhibited by graphene and graphene nanoribbons (GNRs), together with the possibility to be patterned using high-resolution electronic lithography, suggest that these systems have a great potential to be used in new applications in nanotechnology.[1–7] For GNRs, the electronic properties are defined by the quasi-one-dimensional confinement and the shape of the ribbon edges. The two cases of maximum symmetry are known as zigzag graphene nanoribbons (ZGNRs) and armchair graphene nanoribbons (AGNRs). Different approaches to describe the electronic and transport properties of GNRs may be found in the literature such as the massless Dirac equation, *ab initio* schemes, and simple scenarios based on tight-binding models. Each one of these models predicts that all ZGNRs are metallic independently of their width, whereas AGNRs are always semiconductors with three different families of energy gaps depending on its width.[8–14]

Recently, both experimental and theoretical works have addressed the possibility to create on graphene, a single or a few number of vacancies, or even a superlattice (SL) of vacancies (antidots).[15] Distinct kinds of local modulations have been proposed to generate repeated patterns of graphene nanoribbons.[16,17] Some interesting results are related with the magnetic behavior and magnetoconductance oscillations in graphene with antidots; the long-range magnetic order exhibited in graphene with antidots, even at room temperature, indicates that these systems can be natural candidates for spintronics applications and computation.[18–22]

Here we present a theoretical study of the electronic and transport properties of AGNR SLs formed by periodic sequence of vacancies modulated by different geometrical structures and sizes. In Fig. 1 we show the different configurations considered in this study: (a) an hexagon-type defect with six extracted atoms, (b) a symmetric rhomboid-type defect, and (c) an asymmetrical rhomboid-type defect with eight extracted atoms. Strong modulations of the electronic and transport properties of these systems are found. With the presence of the antidots, the electronic band structure and the density of states (DOS) show the apparition of energy gaps and new available electronic states. The energy gap structure is reflected on the conductance of the SLs, which depends on the period, the number of extracted atoms, and the symmetry of the systems. All nanostructures have been relaxed using the direct inversion iterative subspace method[23] with a residual force criteria less than 10^{-4} hartree/bohr. The elec-

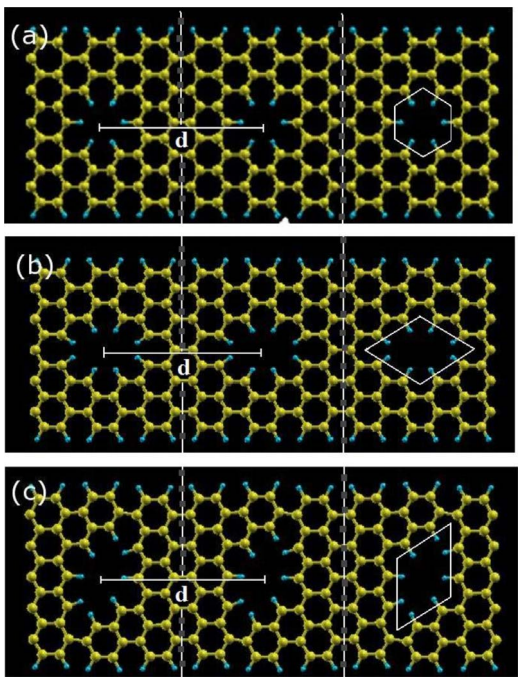

FIG. 1. (Color online) Schematic view of the considered nanoribbon systems; dashed lines marking the interfaces between the conductor and the right and left leads. Each SL is formed by a *N*-AGNR with (a) an hexagon-type defect with six extracted atoms, (b) a symmetric rhomboid-type defect, and (c) an asymmetric rhomboid-type defect with eight extracted atoms. The three panels show the period $d=3$ of the corresponding SL, measured in units of the primitive cell of the pristine AGNR.

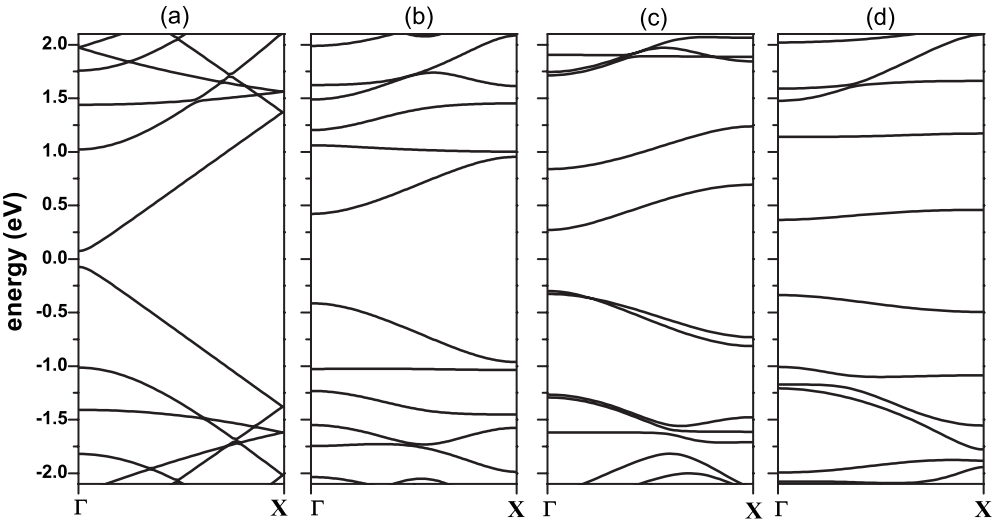

FIG. 2. Electronic band structure of the considered systems: (a) pristine $N=11$ AGNR, (b) hexagon-type of SL, (c) symmetric rhomboid-type of SL, and (d) asymmetric rhomboid-type of SL. All superlattices have the same period $d=3$ measured in units of the primitive cell of the pristine AGNR.

tronic band structure and the DOS of each SL were calculated within *ab initio* calculations based on the pseudopotential method and using the local spin density approximation, taking into account an energy cutoff equal to 150 Ry and a convergence criteria of 10^{-6} hartree at room temperature.[24] The edges of all nanostructures were passivated with hydrogen atoms. Calculations were made using the OPENMX code.[25]

The DOS and the conductance of the considered systems are also calculated within a single-band tight-binding approach. In this scheme, the SLs are described by

$$H_T = \sum_i \varepsilon_i c_i^\dagger c_i + \gamma \sum_{\langle ij \rangle} (c_i^\dagger c_j + \text{H.c.}), \tag{1}$$

where ε_i is the on-site energy (taken as the zero of energies) and $\gamma=2.55$ eV is the hopping parameter, which is extracted from the *ab initio* calculations.

The transport properties of the system are calculated using the surface Green's function matching formalism[17,26,27] based on real-space renormalization techniques. The system is separated in three blocks: a central structure and two semiinfinite leads composed of the same central part that repeats indefinitely, forming a superlattice structure. The central conductor is composed of a number of atoms that depends essentially on the distance d and the type of defect considered. It includes the corresponding vacancy (hexagonal or rhomboidlike defects), located in the middle of the cell. The central part of the conductor for the case of $d=3$ is shown in Fig. 1. Dashed lines mark the interfaces between this central part and the right or left lead.

The conductance is calculated in the linear response approach using the Landauer formalism[28,29] and it is written as

$$G = \frac{2e^2}{h} T(E_F) = \frac{2e^2}{h} \text{Tr}[\Gamma_L G_C^r \Gamma_R G_C^a], \tag{2}$$

where $T(E_F)$ is the transmission function of an electron crossing the central conductor, $G_C^{r(a)}$ is the retarded (advanced) conductor Green's function, $\Gamma_{L,R}=i[\Sigma_{L,R}^r-\Sigma_{L,R}^a]$ are the coupling between the leads and the conductor, and $\Sigma_{L,R}$ are the self-energies of each lead, given by $\Sigma_{L(R)}=(H_{CL(R)})^\dagger g_{L(R)} H_{CL(R)}$, where H_{CL} are the coupling matrix elements between the central conductor and the leads and $g_{L(R)}$ is the surface Green's function of the left (right) semi-infinite lead. In this scheme the DOS can be written as $\text{DOS}(\omega)=-\frac{1}{\pi}\text{Im}\{\text{Tr}[G_C(\omega)]\}$, where Tr is the matrix trace symbol.

Ab initio results of the electronic band structure of superlattices formed by a $N=11$ AGNR and three different types of antidots are shown in Fig. 2. In all cases the number of extracted atoms of each sublattice A and sublattice B of the crystallographic structure is the same. For an appropriate comparison between these systems, we have considered the same unit cell size for each SL. As a reference, we have included the pristine $N=11$ AGNR case. All considered SLs show a semiconductor electronic behavior with a gap structure that depends on the number of extracted atoms, the geometry of the antidots, and the new supercell symmetry. As a result of the additional electronic confining potentials and the new periodicity imposed by the antidots, the band structure of the pristine case is modified. The change in the point group of the pristine unit supercell due to the presence of the vacancies in each SL is manifested as a degeneration breaking of the states at the edge of the unidimensional Brillouin zone (X point). The energy bands for the hexagon-type and the symmetric rhomboid-type vacancy SL structures show a similar behavior as a function of the longitudinal wave vector k. This is due to that both antidot SLs own the same specular symmetry with respect to the longitudinal axis of the nanostructure, and the distance from the defects to the edges of the AGNR is the same in both cases. In other hand, the energy dispersions of both considered rhomboid-type vacancy SLs are very distinct. Despite of the number of extracted atoms in both systems is the same, the band structures show great differences. This is mainly not only due to the lack of specular symmetry with respect to the longitudinal ribbon axis of the asymmetric rhomboid-type SL but also due to the particular geometry of this vacancy for which the distance of the defects with respect to the edges of the ribbon is shorter than in the symmetric rhomboid-type vacancy. Finally, the relative distance between two consecutive antidots in both SLs is different, leading the possibility of distinct electronic states in the systems. This behavior is more evi-

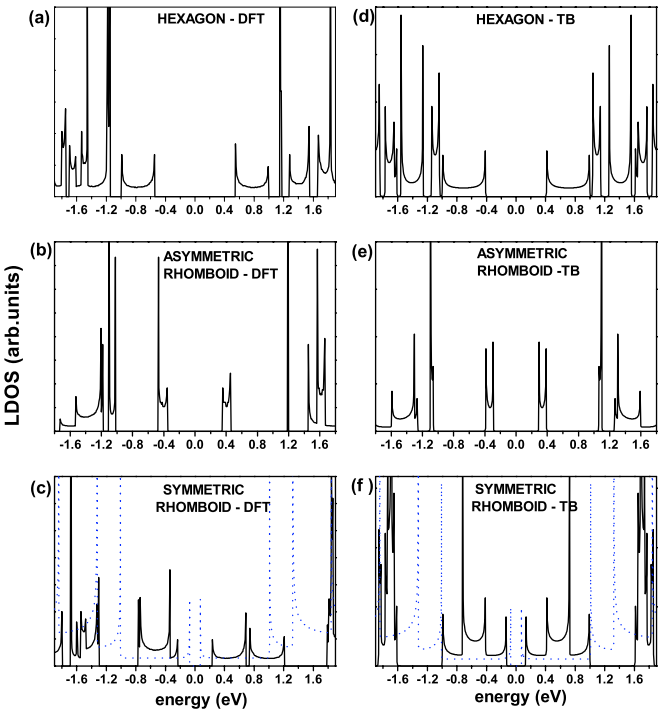

FIG. 3. (Color online) Comparison of the DOS calculated by DFT calculations, displayed in panels (a)–(c), and by a tight-binding Hamiltonian, displayed in panels (d)–(f). All considered SLs have the same period $d=3$. As a reference, the DOS of a pristine $N=11$ AGNR is included in dotted (blue online) curve.

dent in Fig. 3 which displays results of the DOS of each considered SLs on a $N=11$ AGNR obtained by both *ab initio* and tight-binding calculations. All considered SLs have the same period $d=3$. The pristine case of a $N=11$ AGNR is included as a reference (dotted line). Left panels correspond to the *ab initio* calculations, while the right panels correspond to the tight-binding approach. It is clear from Fig. 3 the good agreement in the low energy region between these two different models. These results indicate that calculations of the transport properties of the considered SLs based on a tight-binding approach would be a very good first approximation to describe the low energy electronic behavior of the systems. The DOS of the structures with three types of defects, displayed in Fig. 3, corresponds actually to the mean density of states calculated at the central conductor. All of them exhibit sequences of superimposed one-dimensional density of states, with the characteristic Van Hove singularities. One clearly notices that the DOS is strongly dependent on the defect symmetry and this should be reflected on the transport properties of these structures. The spatial electronic distribution across the superlattice structure may be investigated by calculating the local density of state at different sites of the system. By performing that we note for some energy ranges, the electron wave function is completely localized around the vacancy region, promoting a complete suppression of the transport. Figure 4 shows the behavior of the conductance as a function of the Fermi energy for the three SLs considered above for a period $d=3$ on a $N=11$ AGNR, and for comparison we have included the case of the corresponding $N=11$ AGNR pristine. It can be observed that

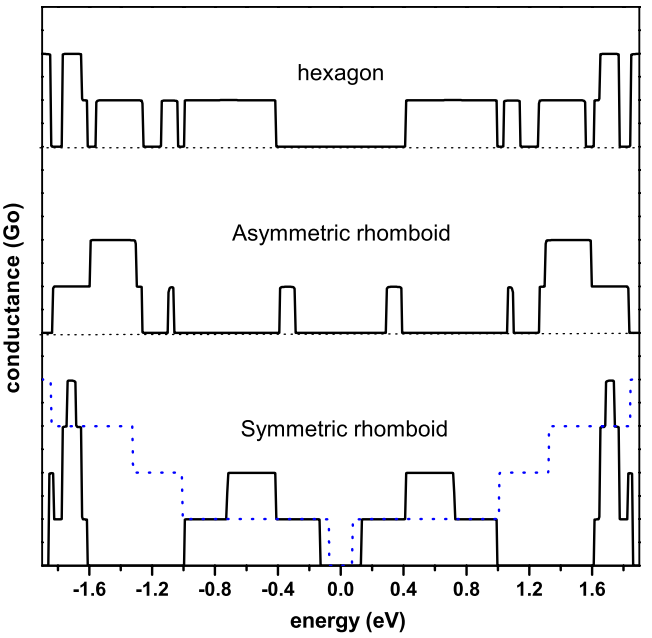

FIG. 4. (Color online) Conductance as a function of the energy for $N=11$ AGNR SLs with period $d=3$. The case of a pristine $N=11$ AGNR is also included as reference. All the curves have been displaced for a better visualization.

for the asymmetric rhomboid-type SL in the energy range between 0.4 and 1.0 eV a total conductance suppression occurs. Otherwise, for the symmetric rhomboid-type SL, a delocalization phenomenon occurs at the same mentioned energy range, promoting an extra channel and a consequent increase in one step in the conductance. We then conclude that by performing different types of defects we can get opposite transport effects, which may be of great importance to tune electronic response in designed devices.

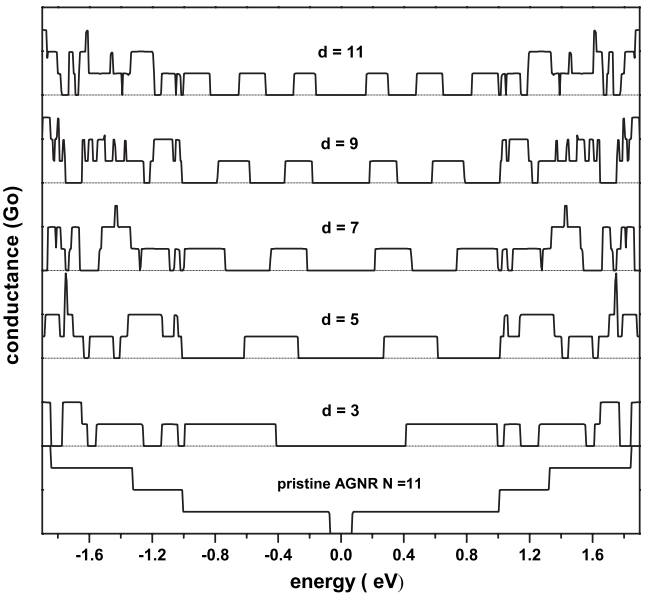

FIG. 5. Conductance as a function of the period d of the hexagon-type antidot superlattice on a $N=11$ AGNR. All curves have been displaced for a better visualization.

Results of the conductance as a function of the period d of an hexagon-type SL on an armchair graphene nanoribbon $N=11$ are shown in Fig. 5. We have considered different values for the period of the SL, $d=3$, 5, 7, 9, and 11. We can observe that for low energies ($|E_F|<1$ eV) the number of minibands increases with the SL period. As this period increases, the size of the unit cell augments, and more resonant states contribute to the conductance in this energy range. For higher energies ($|E_F|>1$ eV) the conductance shows a more complex structure due to the increased number of allowed conductive channels contributing to the transmission.

The obtained results are actually quite similar to the case of transmission through multibarrier systems, in which quantum interference phenomena drive the transport, leading to the formation of minigaps and minibands that are dependent on the number of barrier and the space between them. In the case of traditional semiconducting superlattices,[30] as the distance between the barrier increases, a large number of bands and gaps are obtained in the central energy part of the spectrum, as well as the size of the central gap decreases as d increases. This is exactly what is obtained when the period d is changed in our calculations.

In summary, we have studied the dependence of the electronic and transport properties of AGNR antidot SLs on the details of the geometrical configuration of the systems. The transport behavior of these complex systems is defined by the new electronic energy states and forbidden energy regions which appear due to the extra electronic confinement potential and the new types of symmetries imposed by the periodic vacancies in the lattice. In the actual nanotechnology scenario which guarantees, for instance, the controlled variation in chirality and diameter of carbon nanotubes, leading to the formation of molecular intrajunctions,[31] one certainly believes that investigation like the presented here, even considering the simplicity of the model calculation, is relevant for new proposal of carbon-based device applications.

We acknowledge the financial support of CONICYT/Programa Bicentenario de Ciencia y Tecnología (CENAVA, Grant No. ACT27), UTFSM internal grant, CIAM (CONICYT-CNPq-NSF), Brazilian Agencies CNPq, FAPERJ, Rede Nacional de Nanotubos, and a grant of Instituto do Milênio.

*monica.pacheco@usm.cl

[1] K. S. Novoselov, A. K. Geim, S. V. Morozov, D. Jiang, Y. Zhang, S. V. Dubonos, I. V. Grigorieva, and A. A. Firsov, Science **306**, 666 (2004).
[2] A. C. Ferrari, J. C. Meyer, V. Scardaci, C. Casiraghi, M. Lazzeri, F. Mauri, S. Piscanec, D. Jiang, K. S. Novoselov, S. Roth, and A. K. Geim, Phys. Rev. Lett. **97**, 187401 (2006).
[3] F. Schedin, A. K. Geim, S. V. Morozov, E. W. Hill, P. Blake, M. I. Katsnelson, and K. S. Novoselov, Nature Mater. **6**, 652 (2007).
[4] C. Berger, Z. Song, X. Li, X. Wu, N. Brown, C. Naud, D. Mayou, T. Li, J. Hass, A. N. Marchenkov, E. H. Conrad, P. N. First, and W. A. de Heer, Science **312**, 1191 (2006).
[5] Y. Son, Marvin L. Cohen, and Steven G. Louie, Nature (London) **444**, 347 (2006).
[6] A. Rycerz, J. Tworzydlo, and C. W. J. Beenakker, Nat. Phys. **3**, 172 (2007).
[7] H. B. Heersche, P. Jarillo-Herrero, J. B. Oostinga, L. M. K. Vandersypen, and A. F. Morpurgo, Nature (London) **446**, 56 (2007).
[8] K. Nakada, M. Fujita, G. Dresselhaus, and M. S. Dresselhaus, Phys. Rev. B **54**, 17954 (1996).
[9] K. Wakabayashi, Phys. Rev. B **64**, 125428 (2001).
[10] N. M. R. Peres, A. H. Castro Neto, and F. Guinea, Phys. Rev. B **73**, 195411 (2006).
[11] A. H. Castro Neto, F. Guinea, N. M. R. Peres, K. S. Novoselov, and A. K. Geim, Rev. Mod. Phys. **81**, 109 (2009).
[12] A. Cresti, N. Nemec, B. Biel, G. Niebler, F. Triozon, G. Cuniberti, and S. Roche, Nano Res. **1**, 361 (2008).
[13] Y. W. Son, M. L. Cohen, and S. G. Louie, Phys. Rev. Lett. **97**, 216803 (2006).
[14] L. Brey and H. A. Fertig, Phys. Rev. B **73**, 235411 (2006).
[15] T. G. Pedersen, C. Flindt, J. Pedersen, N. A. Mortensen, A.-P. Jauho, and K. Pedersen, Phys. Rev. Lett. **100**, 136804 (2008).
[16] H. Sevinçli, M. Topsakal, and S. Ciraci, Phys. Rev. B **78**, 245402 (2008).
[17] L. Rosales, M. Pacheco, Z. Barticevic, A. Latgé, and P. A. Orellana, Nanotechnology **20**, 095705 (2009).
[18] K. Wakabayashi, J. Phys. Soc. Jpn. **71**, 2500 (2002).
[19] T. Shen, Y. Q. Wu, M. A. Capano, L. P. Rokhinson, L. W. Engel, and P. D. Ye, Appl. Phys. Lett. **93**, 122102 (2008).
[20] J. J. Palacios, J. Fernandez-Rossier, and L. Brey, Phys. Rev. B **77**, 195428 (2008).
[21] P. H. Rivera, M. A. Andrade Neto, P. A. Schulz, and N. Studart, Phys. Rev. B **64**, 035313 (2001).
[22] D. Yu, E. M. Lupton, M. Liu, W. Liu, and F. Liu, Nano Res. **1**, 56 (2008).
[23] P. Zsaszar and P. Pulay, J. Mol. Struct.: THEOCHEM **114**, 31 (1984).
[24] T. Ozaki, Phys. Rev. B **67**, 155108 (2003); T. Ozaki and H. Kino, *ibid.* **69**, 195113 (2004); **72**, 045121 (2005).
[25] http://www.openmx-square.org
[26] M. Buongiorno Nardelli, Phys. Rev. B **60**, 7828 (1999).
[27] C. G. Rocha, A. Latgé, and L. Chico, Phys. Rev. B **72**, 085419 (2005).
[28] S. Datta, *Transport Properties of Mesoscopic Systems* (Cambridge University Press, Cambridge, 1995).
[29] F. Garcia-Moliner and V. R. Velasco, *Theory of Single and Multiple Interfaces* (World Scientific, Singapore, 1992).
[30] G. Bastard, *Wave Mechanics Applied to Semiconductor Heterostructures* (Les Editions de Physique, Les Ulis, 1988).
[31] Y. Yao, Q. Li, J. Zhang, R. Liu, L. Jiao, Y. T. Zhu, and Z. Liu, Nature Mater. **6**, 283 (2007).